Genomic Profiling of Pediatric Malignant Hematopoietic and Lymphoid Diseases by Next-Generation Sequencing-based Methods and Bioinformatic Approaches

Ph.D. thesis

Gábor Bedics, MD

Pathological Sciences Doctoral School
Semmelweis University

Supervisor: Donát Alpár, PhD

Official reviewers: Gergely Varga, MD, PhD
András Bors, PhD

Head of the Complex Examination Committee:
Monika Csóka, MD, PhD

Members of the Complex Examination Committee:
Gergely Kriván, MD, PhD
Gábor Turu, MD, PhD

Budapest, 2024

1. Introduction

Cancer is a leading cause of mortality among children aged 1 to 14 years in Western countries, surpassed only by accidents; and it is the fourth most common cause of death among adolescents aged 15-19 years. Standardized incidence of pediatric (aged 0-18 years) malignant diseases is approximately 150 per million in Hungary, with around 280 novel diagnoses per year. Malignant diseases of hematopoietic and lymphoid tissues are responsible for 40% of all pediatric malignancies among young children and for one third of malignant diseases in adolescents.

Acute lymphoblastic leukemia (ALL), the most common malignant disease of childhood accounts for 80% of all pediatric leukemia cases and displays B-cell precursor phenotype (B-ALL) in approximately 85% of the patients. Although the overall survival (OS) of B-ALL exceeds 90% in Western countries, integration of novel molecular genetic data and advancements in biotechnology may further facilitate the improvement of patient survival. Current classification (5th edition) of the World Health Organization (WHO) includes 13 B-ALL subgroups determined by presence or absence of (*i*) numerical or subchromosomal DNA copy number aberrations (CNAs), (*ii*) gene rearrangements, or (*iii*) gene expression profiles.

Copy number aberrations such as whole chromosome gains and losses as well as subchromosomal imbalances recurrently occur as primary or secondary alterations, and substantially contribute to the heterogeneous genomic landscape of ALL. The vast majority of numerical chromosome aberrations emerge in the high-hyperdiploid subgroup which accounts for 25-30% of pediatric B-ALL patients, with the leukemic blasts in this

subgroup bearing non-random gains of specific chromosomes conferring a modal chromosome number of 51-67. Subchromosomal CNAs recurrently affect genes involved in cell cycle control, tumor suppression, lymphoid cell development and B-cell differentiation. A wide range of methods is available for screening CNAs in pediatric ALL, including karyotyping, fluorescence *in situ* hybridization (FISH), DNA index measurement, multiplex ligation-dependent probe amplification (MLPA), cytogenomics, optical genome mapping as well as various array- and next-generation sequencing (NGS) based approaches. DigitalMLPA is a recently developed technique which combines MLPA with NGS readout providing a high-throughput, scalable, highly rationalized but still comprehensive means to interrogate recurrently affected genomic loci with a short turn-around time as previously demonstrated by our group and others.

Several studies investigated the clinical significance of CNAs in pediatric ALL and identified a range of prognostic biomarkers based on modal chromosome number, specific trisomies, simultaneous presence and absence of various trisomies, loss or gain/amplification of key driver genes as well as specific alteration patterns of predefined gene sets. These observations facilitated the widespread implementation of CNA screening in the diagnostics of pediatric ALL, with an aim to support patient stratification and potentially aid therapy selection.

Integrative efforts have led to the establishment of complex classifiers enabling the assignment of patients to distinct prognostic subgroups based on cytogenetic and molecular genetic markers. Shortcomings of current genetic classifiers are the relatively low number and limited combinations of aberrations used as criteria for decision making.

Histiocytic and dendritic cell neoplasms are rare tumors originating from common myeloid progenitors and showing differentiation towards cells of the mononuclear phagocyte system, comprising monocytes, macrophages and dendritic cells. Histiocytic neoplasms display macrophage differentiation and include histiocytic sarcoma, Rosai-Dorfman-Destombes disease, ALK-positive histiocytosis, Erdheim-Chester disease, and juvenile xanthogranuloma, albeit this last entity has also been suggested to originate from dermal/interstitial dendritic cells. Histiocytic neoplasms frequently harbor mutations with variable frequencies in genes of the mitogen-activated protein kinase (MAPK) pathway, which suggests a unifying genetic landscape of these diseases.

These genetic features are exploitable by molecularly targeted therapeutic approaches, such as BRAF and MEK inhibitions, which have the potential to effectively target components of the activated signaling pathway, often offering durable responses for the patients.

2. Objectives

During my PhD research, we aimed:

1. To perform comprehensive screening for disease-relevant DNA copy number aberrations in a cohort of Hungarian pediatric patients diagnosed with B-ALL using digitalMLPA, a novel next-generation sequencing-based molecular technique.
2. To analyze co-segregating variants and WHO subgroups, displaying co-occurrence or mutually exclusive appearance in pediatric B-ALL.
3. To scrutinize whole chromosome gains individually and in combinations to identify specific patterns associated with favorable outcome among B-ALL patients with high-hyperdiploid karyotype as revealed or confirmed by digitalMLPA.
4. To analyze *IKZF1* status at exon level (provided by digitalMLPA method) and combine *IKZF1* status (*IKZF1*^{normal}, *IKZF1*^{del} and *IKZF1*^{plus}) with cytogenetic classes, thus creating a cytogenetics aware interpretation of *IKZF1* imbalance in pediatric B-ALL.
5. To introduce a conceptually novel patient classification approach, which assigns B-ALL patients to prognostic subgroups based on highly individualized cumulative scores reflecting the weighted impact of all relevant aberrations detected in a particular patient.
6. To validate our findings regarding the detected CNAs and the conceptually novel patient classification approach for pediatric B-ALL on a large-scale independent validation cohort with *in-silico* approach.
7. To perform comprehensive genetic characterization and relevant orthogonal validation analyses on the first *ROS1* translocated histiocytic neoplasm sample.

8. To assess clinicopathological features and success of a molecularly targeted therapeutic attempt with ROS1-inhibitor entrectinib with off-label indication on the first patient diagnosed with *ROS1* translocated histiocytic neoplasm.

3. Methods

3.1. Comprehensive copy number aberration profiling of pediatric acute lymphoblastic leukemia

3.1.1. Patient samples

In the frame of the Hungarian Pediatric Leukemia Molecular Profiling Program, diagnostic bone marrow samples from 260 patients diagnosed with B-cell precursor ALL were investigated. Diagnoses were made based on morphological, immunophenotypical and genotypical criteria in the Department of Pathology and Experimental Cancer Research, Semmelweis University, in the Department of Pathology, University of Pécs, or in the Department of Pathology, University of Debrecen between 2003 and 2019. Specimens contained on average 79% leukemic blasts as assessed by flow cytometry. Baseline genetic characterization of patient samples included DNA index measurement by flow cytometry, karyotyping by GTG-banding, FISH, as well as quantitative PCR tests and conventional MLPA using the SALSA 202 and 335 probemixes (MRC-Holland, Amsterdam, the Netherlands). Risk assessment and treatment selection were performed according to ALL IC-BFM protocols, such as the ALL IC-BFM 2002 (121 patients, 47%) and ALL IC-BFM 2009 (139 patients, 53%). Ethical approval (45563-2/2019/EKU) from the Medical Research Council of Hungary and written informed consent from the patients and/or from the parents or guardians were obtained for the study, which was conducted in accordance with the Declaration of Helsinki.

3.1.2. digitalMLPA

DigitalMLPA reactions were performed on 40 ng genomic DNA using the D007 ALL probemix (version D007-X2-0516 or D007-X5-0220), which was developed by the MRC-Holland

and provided to collaborating laboratories for testing and validation. The probemix consisted of (*i*) target probes for regions recurrently altered by copy number aberrations in acute lymphoblastic leukemia; (*ii*) digital karyotyping probes covering all chromosome arms for detection of gross chromosomal aberrations and serving as reference probes for data normalization, and (*iii*) internal control probes for quality control and sample identification.

DigitalMLPA reactions were carried out according to the previously published protocol. Copy number status at each interrogated locus was determined from the NGS output in two consecutive steps using the Coffalyser digitalMLPA software v.004 (MRC Holland). CNAs were reported as being subclonal if multiple consecutive probes had dosage quotients unambiguously falling outside the normal range but without reaching the expected level of monoallelic loss as calculated based on sample purity, and also compared with other altered regions within the same specimen.

3.1.3. Validation cohort - origin and analysis

The independent validation cohort comprised 606 patients included in the Acute Lymphoblastic Leukemia Pilot Phase 1 (phs0000463) or the Expansion Phase 2 (phs000464) studies of the Therapeutically Applicable Research to Generate Effective Treatments - TARGET initiative.

3.1.4. Statistical analysis

Co-segregations of disease-relevant CNAs were analyzed using the “somaticInteraction” function of maftools Bioconductor package (v2.2.10). EFS up to 5 years was defined as the time from start of treatment to relapse, second malignancy or disease-related death, excluding early toxicity. Mean follow-up time was 46.6 months (range: 1.5-72.0 months) with at least 24.0 months

at patients experiencing no event during the study period. Cox regression models were used for assessing the association of individual genetic aberrations with risk of progression and for building models for progression prediction. Survival rates were estimated using the Kaplan-Meier method and compared by log-rank tests coupled with Benjamini-Hochberg false discovery rate correction. Statistical analyses were performed using R version 4.1.2 (R Foundation for Statistical Computing, Vienna, Austria, 2021).

3.2 Discovery and comprehensive genomic profiling of the first histiocytic neoplasm with *ROS1* gene fusion

3.2.1. Clinical symptoms and histopathological features

A 19-month-old boy presented with visual disturbances as well as vertical nystagmus of the left eye and unstable gait. Magnetic resonance imaging (MRI) revealed multiple subcortical and periventricular white matter lesions also affecting the corpus callosum. One single, larger, homogenously contrast-enhancing, dural-based lesion was described in the right cerebellar hemisphere and another intradural extramedullary lesion in the level of the dens axis. Biopsy was taken from the cerebellar lesion to explore the nature of the disease. Histology showed a dense infiltrate of neoplastic histiocytes in the cerebellar parenchyma and leptomeningeal surface. Tumor cells showed diffuse positivity with CD68 and S100 immunohistochemistry, while CD1a, langerin (CD207), and BRAF p.V600E reactions were negative. Focal strong positivity was detected with D5F3 ALK immunohistochemistry, but rearrangement affecting the *ALK* gene was not detected by FISH. The final histological diagnosis was histiocytic neoplasm (non-Langerhans cell histiocytosis) with some morphological features of juvenile xanthogranuloma.

This research project was conducted in accordance with the Scientific and Research Committee of the Medical Research Council license IV/51-1/2022/EKU.

3.2.2. Comprehensive Genomic Profiling

Genomic DNA and total RNA were isolated from formalin-fixed and paraffin-embedded (FFPE) specimens using the QIAmp DNA FFPE Tissue Kit (QIAGEN GmbH, Hilden, Germany) and the High Pure FFPET RNA Isolation Kit (Roche Diagnostics GmbH, Mannheim, Germany). Library preparation workflow of Illumina TruSight Oncology 500 High Throughput assay was performed according to the manufacturer's protocol. Next-generation sequencing was performed on Illumina NextSeq 2000 platform, with 101-cycle paired-end chemistry. Bioinformatic analysis was performed using the Illumina TruSight Oncology 500 Local App v2.1. For further clinical interpretation, QIAGEN Clinical Insight (QCI) Interpret software was used, which applies variant filtering and further annotations: pathogenicity scores, population-frequency, protein structure predictions, relevant clinical guidelines and therapeutic options for variants.

4. Results

4.1. Comprehensive DNA copy number aberration profiling in pediatric acute lymphoblastic leukemia

4.1.1. Frequency and distribution of chromosomal and subchromosomal DNA copy number aberrations

In total, 1,398 CNAs including gross chromosomal alterations and subchromosomal lesions were detected in 244/260 (93.8%) diagnostic patient samples. On average, 5.4 CNAs were observed per patient with a mean of 2.5 subchromosomal aberrations. Ninety percent of whole chromosome changes were observed in patients bearing hyperdiploid karyotype with 4-14 affected chromosomes, predominantly extra copies of chromosomes 21, 6, X, 14, 18, 17, 4 and 10. Gain of multiple copies was recurrently observed at chromosomes 21, X, 14 and 18. Modal chromosome number among the 82 patients harboring high-hyperdiploid karyotype ranged between 51 and 62 with a median of 55, while one patient displayed near-triploidy with 72 chromosomes.

Subchromosomal CNAs were identified in 208/260 (80.0%) patients, with *VPREB1* deletion being the most common lesion occurring in 32.3% of the cases. Additional genes altered with a frequency of at least 5% in our patient cohort included various cell cycle control, lymphoid development, signaling or tumor suppressor genes such as *CDKN2A/B, ETV6, PAX5, IKZF1, MLLT3, TBL1XR1, BTG1, RB1, BTLA/CD200, CASP8AP2, RUNX1* as well as the PAR1 region.

4.1.2. Co-segregation analysis of various CNAs and genetic subtypes in B-ALL

Simultaneous presence of various CNAs and B-ALL subgroup defining alterations was investigated in order to reveal potential associations between various genetic lesions and B-ALL subgroups.

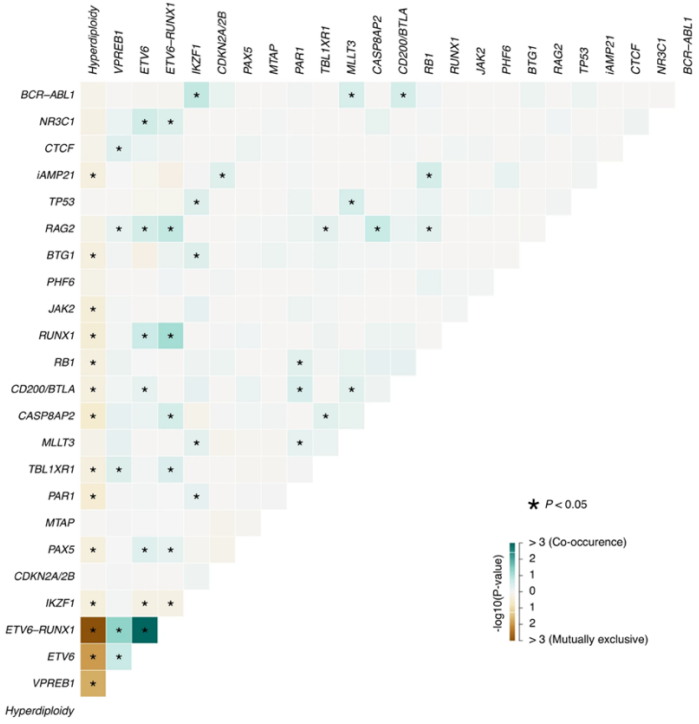

Figure 1. Co-segregation analysis of genetic subgroup defining alterations and copy number aberrations affecting genes recurrently altered in pediatric B-ALL. Co-occurrence and mutual exclusivity between various B-ALL subgroup defining alterations and/or detected copy number aberrations are labeled with green and brown colors, respectively. Significant ($p < 0.05$) associations revealed by pair-wise Fisher's exact test are marked with asterisks.

The vast majority of mutual exclusivity or negative correlations was observed in the high-hyperdiploid subgroup, while the pairwise analyses revealed several significant positive correlations across various disease subtypes (Figure 1).

The strongest positive associations were observed in the *ETV6::RUNX1* subgroup and included *ETV6* loss, *RUNX1* gain and *VPREB1* loss. Among patients with iAMP21, enrichment of *CDKN2A/B* loss and *RB1* deletion was observed. *IKZF1, MLLT3* and *CD200/BTLA* losses were associated with *BCR::ABL1* positivity, while *IKZF1* loss showed negative correlation with *ETV6::RUNX1* fusion and hyperdiploidy. Beyond that, *IKZF1* deletion showed significant co-occurrence with *TP53, BTG1* and *MLLT3* as well as with deletion of the *PAR1* region (Figure 1).

4.1.3. Hyperdiploidy and prognosis

Whole chromosome gains were investigated individually and in combinations to identify specific patterns associated with favorable outcome among patients with high-hyperdiploid karyotype as revealed or confirmed by digitalMLPA. Simultaneous survival rate analyses using the Kaplan-Meier method unraveled multiple single, double and triple trisomies as markers of good risk. After multiple statistical comparisons of these combinations, results were corrected using the Bonferroni method, which unraveled double trisomy of chromosomes 4 and 6 remained as the only marker significantly associated with superior outcome within the high-hyperdiploid subgroup.

4.1.4. IKZF1 status and its prognostic value

The D007 digitalMLPA probemix covers all exons of the *IKZF1* gene with two probes, as well as regions located approximately 4 and 2 kilobases upstream of the coding sequences, enabling a fine mapping of deletions affecting the *IKZF1* gene. In patients harboring *IKZF1* loss, 10 different patterns of deletion were

observed, predominantly exons 4-7 and exons 1-7 losses, as well as deletion of the entire gene including the upstream region (Figure 2). Notably, we observed a non-random distribution of *IKZF1*^{del} and *IKZF1*^{plus} statuses across patients displaying different patterns of *IKZF1* deletion. Eight out of nine patients with exons 4-7 loss and 6/7 patients with upstream region/exons 1-8 (i.e. whole *IKZF1*) deletion showed *IKZF1*^{plus} CNA profile. On the other hand, all patients with exon 1-7 deletion belonged to the *IKZF1*^{del} group, without meeting the criteria of *IKZF1*^{plus}.

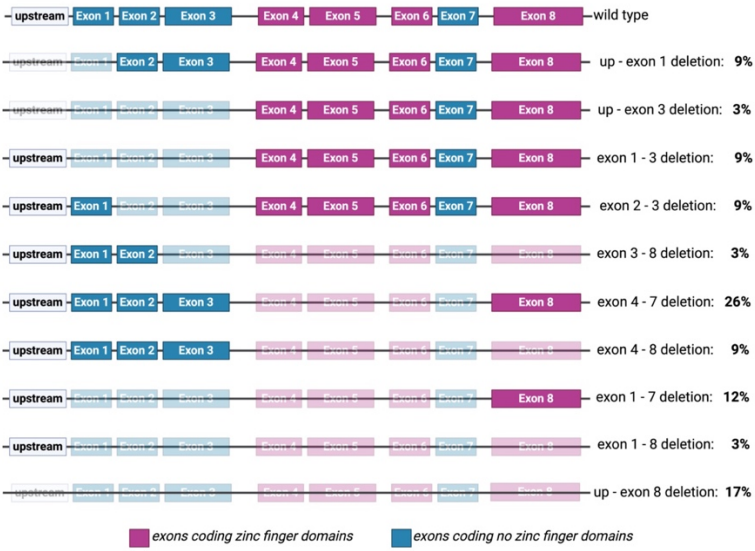

Figure 2. Patterns and frequencies of *IKZF1* gene deletions in children with B-ALL.

By analyzing the prognostic value of *IKZF1* status in our patient cohort, a decreasing rate of EFS was observed in patents with normal vs *IKZF1*^{del} vs *IKZF1*^{plus} genotype; however, the difference between the latter two categories did not reach statistical significance. We hypothesized that co-evaluation of *IKZF1* status and additional cytogenetic features

interdependently may improve the *IKZF1*-driven prognostic risk assessment. In order to generate these novel subgroups, we combined the *IKZF1* status with cytogenetic categories defined and applied successfully in previous studies, which eventually allowed for distinguishing three prognostic groups (IKAROS-low, IKAROS-medium and IKAROS-high) with significantly different 5-year EFS.

4.1.5. Integrative genetic classification for personalized risk assessment

In order to establish a highly personalized risk assessment of patients with B-cell precursor ALL, we introduced a novel classification called *PersonALL*, which flexibly takes account of the unique composition of aberrations in individual patients. First, prognostic significance of all disease-relevant, recurrent genetic aberrations detected by digitalMLPA or by conventional approaches such as karyotyping and FISH was evaluated in our patient cohort using univariate Cox proportional hazard models. Second, aberrations with a frequency of >1.5% and a Cox model hazard ratio of >1.5 or ≤0.66 were selected and used for calculating patient-specific cumulative scores. The scoring system proportionally weighted individual cytogenetic aberrations and subchromosomal CNAs.

Patient-specific cumulative scores generated from the prognostic value of single genetic lesions distinguished four prognostic subgroups with excellent (score: ≥4), good (score: 0-3), high (score: -1 to -4) and ultra-poor risk (score: ≤ -4), demonstrating significantly different 5-year EFS rates (Figure 3).

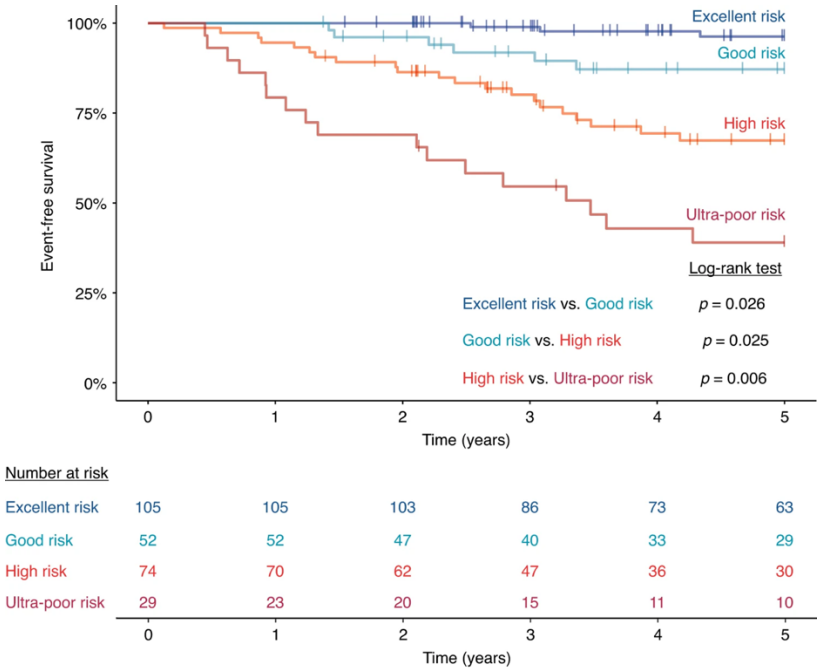

Figure 3: Event-free survival of 260 patients with B-cell precursor ALL, classified according to patient-specific composition of all disease-relevant aberrations associated with prognostic significance in our patient cohort. Excellent, good, high and ultra-poor risk groups showed an estimated 5-year EFS rate of 96.3%, 87.2%, 67.4% and 39.0%, respectively.

The excellent, good, high and ultra-poor risk groups comprised 40.4%, 20.0%, 28.5% and 11.1% of the patients, respectively. The excellent risk group almost exclusively contained patients with *ETV6::RUNX1* fusion or high-hyperdiploid karyotype with common double trisomy of chromosomes 4 and 6. An increased fraction of B-other cases coupled with reduced representativity of *ETV6::RUNX1* positivity and high-hyperdiploidy was observed in the good-risk group. In the high-risk group, almost two-thirds of the patients were classified as B-other, while the ultra-poor risk group was enriched for *BCR::ABL1* chimera gene, and other gene fusions including *CRLF2* and *ABL* class

aberrations characteristic of Ph-like signature and iAMP21 genotype.

Performance of *PersonALL* was validated on an independent cohort of 606 patients included in the TARGET ALL phase 1 pilot and phase 2 expansion studies, using a scoring scheme identical to the one applied at our in-house discovery cohort. Comparison of the excellent, good, high and ultra-poor risk groups consisting of 30.0%, 24.1%, 39.6% and 6.3% of the patients, respectively, demonstrated significantly different 5-year EFS rates. In addition, we tested this novel risk assessment method on the merged dataset comprising relevant information from all patients (n = 866) included in the validation cohort and in our discovery cohort. The difference in 5-year EFS across the risk groups showed even higher statistical significance than observed in the validation cohort, thus providing further confirmation on the value and robustness of our newly introduced prognostic classifier.

4.2 Discovery, comprehensive genomic profiling and effective molecularly targeted therapy of the novel type of histiocytic neoplasm driven by *GIT2::ROS1* gene fusion

4.2.1. Identification of the first histiocytic neoplasm with ROS1 gene fusion by comprehensive genomic profiling

Histopathological diagnosis of the investigated case was histiocytic neoplasm with some morphological features of juvenile xanthogranuloma, however histology and immunophenotype of the tumor overlaps with Erdheim-Chester disease, and ALK-positive histiocytosis. Next-generation sequencing-based comprehensive genomic profiling was performed on FFPE specimen using the Illumina TruSight Oncology 500 assay. Bioinformatic analyses identified a novel

GIT2::ROS1 fusion involving the *GIT2* (12q24.11; exon 16) and *ROS1* (6q22.1; exon 36) loci. The detected fusion was validated using *ROS1* break-apart FISH probe and Sanger sequencing of the fusion transcripts. Comprehensive genomic profile of the analyzed FFPE sample revealed several small nucleotide variants (SNVs), small insertions, deletions (InDels) as well as low-level copy number gains, all of which are considered as variants with unknown clinical significance. Therefore, the detected *GIT2::ROS1* fusion was the only pathogenic variant, hence driver genetic event in the sample.

4.2.2. Effective therapeutic targeting of the driver ROS1 gene fusion conferred favorable clinical outcome

The treatment was started with the DAL-HX 90 chemotherapeutic regimen including alternating "A" (etoposide, ifosfamide and methotrexate) and "B" (vinblastine, etoposide and methotrexate) blocks, completed with intrathecal triple therapy (methotrexate, prednisolone and cytarabine) and subcutaneous cladribine (Figure 4). Following these, entrectinib treatment was applied as a maintenance therapy based on the molecular report, with an off-label indication. Control MRI performed during the chemotherapy as well as 1 month and 4 months following the introduction of entrectinib showed radiologically stable disease. In the second month of entrectinib treatment, clear improvement of visual disturbances was clinically detectable, although a visual field defect of the right eye was suspected and the nystagmus was still present. Six months following the entrectinib treatment initiation, by the time of the submission of the publication (Bedics, Csóka et. al.: Novel actionable *ROS1::GIT2* fusion in non-Langerhans cell histiocytosis with central nervous system involvement, Acta Neuropathologica, 2022), the visual field defect was no longer

evident, and the patient could show parts of tiny objects and imitate the examiner's gesticulation.

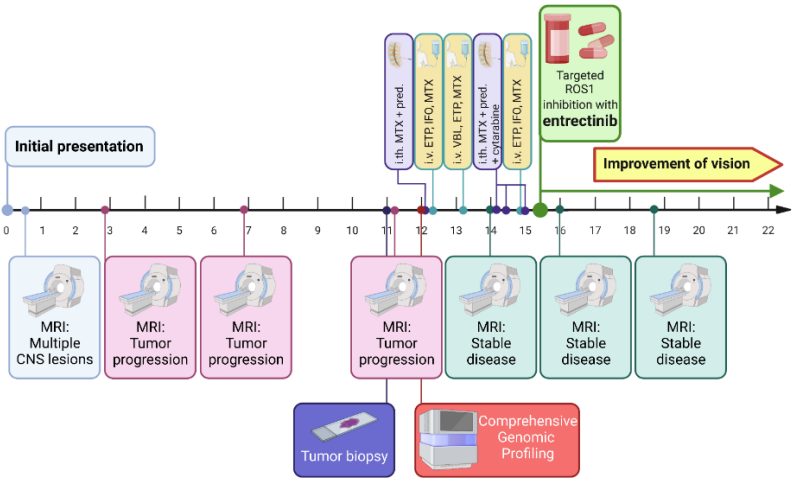

Figure 4. Timeline demonstrating the diagnostic procedures and therapeutic interventions during the clinical course of the reported case in months from the initial presentation (CNS: central nervous system, ETP: etoposide, IFO: ifosfamide, i.th.: intrathecal, i.v.: intravenous, MRI: magnetic resonance imaging, MTX: methotrexate, pred.: prednisolone, VBL: vinblastine)

5. Conclusions

Novel findings of my thesis are the following:

1. We determined a comprehensive disease-relevant DNA copy number aberration profile applying digitalMLPA, a robust high-throughput method in a large cohort of Hungarian children diagnosed with B-ALL (N=260, representing patient number equivalent with 4-year-incidence in Hungary) for the first time.
2. We observed a strong association of specific deletion patterns with either *IKZF1*^{del} or *IKZF1*^{plus} genotype. Importantly, almost all patients harboring exon 4-7 deletion showed *IKZF1*^{plus} genotype leading to the loss of DNA binding region of the protein, which can provide a plausible explanation why this lesion is typically associated with very adverse clinical outcome. Moreover, all patients with exon 1-7 deletion belonged to the *IKZF1*^{del} group, without meeting the criteria of *IKZF1*^{plus}.
3. We integrated *IKZF1* status (*IKZF1*^{normal}, *IKZF1*^{del} and *IKZF1*^{plus}) as revealed by digitalMLPA with cytogenetic classes for the first time, thus creating a cytogenetics aware interpretation of *IKZF1* allelic status, which substantially improved the risk assessment for our patients by distinguishing three prognostic groups with significantly different 5-year EFS.
4. We introduced a conceptually novel genetic risk classification approach called *PersonALL*, which assigns patients to prognostic subgroups based on highly individualized cumulative scores reflecting the weighted impact of all relevant aberrations detected in

a particular patient. This newly developed prognostic classifier which flexibly considers all possible combinations of screened and potentially co-segregating genetic alterations provides a more refined, hence more personalized risk assessment for children with B-ALL.

5. We discovered the first histiocytic neoplasm driven by a novel *ROS1* gene fusion (*GIT2::ROS1*) identified by comprehensive genomic profiling and validated by various orthogonal molecular laboratory methods.
6. We provided the first evidence of efficacious ROS1-inhibitor treatment in the patient diagnosed with *ROS1*-translocated histiocytic neoplasm, with significant improvement of clinical symptoms and achievement of a radiologically stable disease.

6. Bibliography of the candidate's publications

Publications related to the thesis:

Bedics G*, Egyed B*, Kotmayer L, Benard-Slagter A, de Groot K, Bekő A, Hegyi LL, Bátai B, Krizsán S, Kriván G, Erdélyi DJ, Müller J, Haltrich I, Kajtár B, Pajor L, Vojcek Á, Ottóffy G, Ujfalusi A, Szegedi I, Tiszlavicz LG, Bartyik K, Csanádi K, Péter G, Simon R, Hauser P, Kelemen Á, Sebestyén E, Jakab Z, Matolcsy A, Kiss C, Kovács G, Savola S, Bödör C, Alpár D. PersonALL: a genetic scoring guide for personalized risk assessment in pediatric B-cell precursor acute lymphoblastic leukemia. Br J Cancer. 2023 Aug;129(3):455-465. (* joint first author)

Bedics G*, Csóka M*, Reiniger L, Varga E, Liptai Z, Papp G, Bekő A, Cervi C, Bödör C, Scheich B. Novel actionable ROS1::GIT2 fusion in non-Langerhans cell histiocytosis with central nervous system involvement. Acta Neuropathol. 2023 Jan;145(1):153-156. (* joint first author)

Publications unrelated to the thesis:

Bedics G, Kotmayer L, Zajta E, Hegyi LL, Brückner EÁ, Rajnai H, Reiniger L, Bödör C, Garami M, Scheich B. Germline MUTYH mutations and high-grade gliomas: Novel evidence for a potential association. Genes Chromosomes Cancer. 2022 Oct;61(10):622-628.

Bedics G, Szőke P, Bátai B, Nagy T, Papp G, Kránitz N, Rajnai H, Reiniger L, Bödör C, Scheich B. Novel, clinically relevant genomic patterns identified by comprehensive genomic profiling in ATRX-deficient IDH-wildtype adult high-grade gliomas. Sci Rep. 2023 Oct 27;13(1):18436.

Bedics G, Sebestyén E, [Basic concepts of diagnostic application of next-generation sequencing – a practical introduction to precision medicine], Orvosképzés 96 : 3 pp. 343-355. , 13 p. (2021), (Hungarian)

Jia X, Gábris F, Jacobsen Ó, Bedics G, Botz B, Helyes Z, Kellermayer Z, Vojkovics D, Berta G, Nagy N, Jakus Z, Balogh P. Foliate Lymphoid Aggregates as Novel Forms of Serous Lymphocyte Entry Sites of Peritoneal B Cells and High-Grade B Cell Lymphomas. J Immunol. 2020 Jan 1;204(1):23-36.

Kellermayer D, Tordai H, Kiss B, Török G, Péter DM, Sayour AA, Pólos M, Hartyánszky I, Szilveszter B, Labeit S, Gángó A, Bedics G, Bödör C, Radovits T, Merkely B, Kellermayer MS. Truncated titin is structurally integrated into the human dilated cardiomyopathic sarcomere. J Clin Invest. 2024 Jan 16;134(2):e169753.

Jenei A, Bedics G, Erdélyi DJ, Müller J, Györke T, Bödör C, Szepesi Á. Potential role of MAP2K1 mutation in the trans-differentiation of interdigitating dendritic cell sarcoma: Case report and literature review. Front Pediatr. 2022 Sep 16;10:959307.

Varadi M, Nagy N, Reis H, Hadaschik B, Niedworok C, Modos O, Szendroi A, Ablat J, Black PC, Keresztes D, Csizmarik A, Olah C, Gaisa NT, Kiss A, Timar J, Toth E, Csernak E, Gerstner A, Mittal V, Karkampouna S, Kruithof de Julio M, Gyorffy B, Bedics G, Rink M, Fisch M, Nyirady P, Szarvas T. Clinical sequencing identifies potential actionable alterations in a high rate of urachal and primary bladder adenocarcinomas. Cancer Med. 2023 Apr;12(7):9041-9054.

Krizsán S, Péterffy B, Egyed B, Nagy T, Sebestyén E, Hegyi LL, Jakab Z, Erdélyi DJ, Müller J, Péter G, Csanádi K, Kállay K, Kriván G, Barna G, Bedics G, Haltrich I, Ottóffy G, Csernus K, Vojcek Á, Tiszlavicz LG, Gábor KM, Kelemen Á, Hauser P, Gaál Z, Szegedi I, Ujfalusi A, Kajtár B, Kiss C, Matolcsy A, Tímár B, Kovács G, Alpár D, Bödör C. Next-Generation Sequencing-Based Genomic Profiling of Children with Acute Myeloid Leukemia. J Mol Diagn. 2023 Aug;25(8):555-568.

Sztankovics D, Krencz I, Moldvai D, Dankó T, Nagy Á, Nagy N, Bedics G, Rókusz A, Papp G, Tőkés AM, Pápay J, Sápi Z, Dezső K, Bödör C, Sebestyén A. Novel RICTOR amplification harbouring entities: FISH validation of RICTOR amplification in tumour tissue after next-generation sequencing. Sci Rep. 2023 Nov 10;13(1):19610.

Lippai Z, Péterfia B, Papp G, Dezső K, Bedics G, Pápai Z, Lamers MH, Kuin RC, Szuhai K, Sápi Z. A recurrent NTRK1 tyrosine kinase domain mutation pair is characteristic in a subset of dedifferentiated liposarcomas. Eur J Cancer. 2024 May;202:114005.

Cervi C, Sápi Z, Bedics G, Zajta E, Hegyi L, Pápay J, Dezső K, Varga E, Mudra K, Bödör C, Csóka M. Case report: Complete and durable response to larotrectinib (TRK inhibitor) in an infant diagnosed with angiosarcoma harbouring a KHDRBS1-NTRK3 fusion gene. Front Oncol. 2023 Feb 23;13:999810.

Brückner E, Bedics G, Reiniger L, Rajnai H, Jakab Z, Bödör C, Scheich B, Garami M. [Childhood brain tumors: diagnosis and therapy - comprehensive genomic profiling], Magyar Onkológia 67 : 4 pp. 315-320. , 6 p. (2023), (Hungarian)

Szabó S, Bedics G, Bödör C, Csóka M. [Tumor agnostic therapy in pediatric oncology], Klinikai Onkológia 10 : 2 pp. 127-132. , 6 p. (2023), (Hungarian)

Brückner E, Bedics G, Rajnai H, Bödör C, Garami M. [The role of comprehensive genomic profiling in the design of therapy for childhood brain tumours], Gyermekgyógyászat 72 : 6 pp. 429-434. , 6 p. (2021), (Hungarian)

∑IF: 79.522